Carbohydrate- and Chain Length-Controlled Complexation of Carbon Nanotubes by Glycopolymers

Michael A. Cantwell,[1,†] Ka Keung Chan,[2,†] Xue-Long Sun,[1,2,] Geyou Ao[1,]**

[1]Department of Chemical and Biomedical Engineering, Washkewicz College of Engineering, Cleveland State University, 2121 Euclid Avenue, Cleveland, OH 44115, USA

[2]Department of Chemistry, Center for Gene Regulation in Health and Disease (GRHD), Cleveland State University, 2121 Euclid Avenue, Cleveland, OH 44115, USA

Corresponding Authors

*g.ao@csuohio.edu; x.sun55@csuohio.edu

Author Contributions

†M.A.C. and K.K.C. contributed equally.

ABSTRACT

Stable dispersions of single-wall carbon nanotubes (SWCNTs) by biopolymers in aqueous environment facilitate their potential biological and biomedical applications. In this report, we investigated a small library of precision synthesized glycopolymers with monosaccharide and disaccharide groups for stabilizing SWCNTs *via* non-covalent complexation in aqueous condition. Among the glycopolymers tested, disaccharide lactose-containing glycopolymers demonstrate effective stabilization of SWCNTs in water, which strongly depends on carbohydrate density and polymer chain length as well. The introduction of disaccharide lactose potentially makes glycopolymers less flexible as compared to those containing monosaccharide and facilitates the wrapping conformation of polymers on the surface of SWCNTs while preserving intrinsic photoluminescence of nanotubes in the near-infrared. This work demonstrates the synergistic effects of the identity of carbohydrate pendant groups and polymer chain length of glycopolymers on stabilizing SWCNTs in water, which has not been achieved previously.

INTRODUCTION

Single-wall carbon nanotubes (SWCNTs) have gained tremendous attention for both material and biomedical research and applications, such as bioimaging, biosensor, and drug delivery applications.[1–8] Particularly, semiconducting SWCNT species have well-defined electronic structures and optical properties, as well as fluoresce in the near-infrared (NIR), an important spectral regime where attenuated tissue autofluorescence and deep tissue penetration occur in biological samples.[3,9,10] However, obtaining effective dispersions of individual SWCNTs in aqueous environments has been a major challenge given that it is the prerequisite for their processing and specific applications *in vivo*. During the past decades, different ways and means, including covalent and non-covalent methods, have been explored for dispersing SWCNTs in water. Covalent modification of SWCNTs often causes permanent change in the carbon lattice, from sp^2 to sp^3 orbital hybridization that may result in optical, electrical, and mechanical deterioration.[11,12] Non-covalent wrapping with surfactants, peptides, and polymers have been found to be a simple way of stabilizing SWCNTs in water.[2,9,13–17] The wrapping of SWCNTs by polymers driven by the synergy of many interactions, such as van der Waals attractions, multivalent π-π stacking, and hydrophobic interactions, presumably enhance the aqueous solubility of SWCNTs without disrupting the π-system of the tube. Some conjugated polymers showed significantly higher energy of interaction with nanotubes compared to that of small molecules leading to better solubilization of SWCNTs in solvents.[14] Furthermore, creating water-soluble polymer-wrapped SWCNT complexes utilizing biocompatible, biomimetic and biological active polymers will provide vast potentials in biological and biomedical research and application.

The basis for the wrapping mechanism of polymers on the surface of SWCNTs *via* non-covalent complexation in liquid media has been the subject of many studies. The formation of a

well-ordered DNA structure wrapped around SWCNTs has been demonstrated extensively by both computational[18–20] and experimental work leading to comprehensive carbon nanotube sorting[21–23] and developing novel optical sensors of biomolecules.[1,24–26] In addition, molecular dynamics simulations of natural polysaccharides, such as chitosan and amylose chains, and SWCNTs in aqueous environments revealed the encapsulation of nanotubes *via* the helical wrapping conformation.[27,28] Experimental work on imaging of SWCNTs complexed with polysaccharides also suggested a helical coating pattern.[15,29] The helical wrapping of SWCNTs has been accounted for many interactions including van der Waals attraction and hydrophobic interactions between polysaccharides and SWCNTs, as well as possible hydrogen-bonding in carbohydrates that stabilizes the helical motif. Aqueous dispersions of polysaccharide-SWCNT complexes are further stabilized due to the hydrophilic hydroxyl groups of carbohydrates being exposed to water.[27,28]

Glycopolymers, namely polymers with carbohydrate pendant groups, have been extensively used as glycoconjugate mimetics for different biological applications.[30–32] It is generally accepted that synthetic glycopolymers can mimic the functions of naturally occurring glycoconjugates[33,34] and have been employed for biosensor and drug delivery applications and bio-functionalization of nanomaterials of different interests.[33,35] Non-covalent complexation of SWCNTs by glycopolymers is of interest due to the potential of polymer backbone to form a wrapping structure on the nanotube surface, while hydrophilic groups being exposed to water for entropic stabilization of polymer-SWCNT complexes. Synthetic glycopolymers also provide greater structural tunability compared to natural glycoconjugates. Therefore, glycopolymers are of choice for producing stable aqueous dispersions of SWCNTs. However, the interplay of both the carbohydrate pendant groups and polymer chain length on creating stable carbohydrate-coated

SWCNT complexes in aqueous environments has not been explored previously. Herein, we report a systematic design of glycopolymers of various chain lengths having different sugars for stable aqueous dispersions of SWCNTs. Specifically, the same polymer scaffold (i.e., polyacrylamide backbone) was functionalized with monosaccharide and disaccharide groups to produce a total of fourteen glycopolymers with different carbohydrate ligand densities and polymer chain lengths. We found that carbohydrate ligand density and polymer chain length play a synergistic role in interactions with SWCNTs and creating stable glycopolymer-wrapped SWCNT complexes in water that incorporate the NIR fluorescence of nanotubes and the unique carbohydrate functionality of glycopolymers. Additionally, the distinct complexation of glycopolymers and SWCNTs was examined by monitoring the optical modulation of glycopolymer-SWCNT complexes upon interacting with surfactants and single-stranded DNA. Our findings provide important insights into creating stable, water-soluble SWCNT complexes with carbohydrate functionalities that can be potentially utilized as fluorescent probes in biological applications, such as profiling specific carbohydrate-protein interactions.

EXPERIMENTAL SECTION

Synthesis of Glycopolymers. All solvents and reagents were purchased from Sigma-Aldrich (USA) and were used as received. Deionized (DI) water with a resistivity of 18 MΩ cm was used as solvent in all reactions and dialysis experiments. Biomimetic glycopolymers with monosaccharide and disaccharide groups were synthesized *via* cyanoxyl free radical-mediated polymerization (CFRMP) scheme in one-pot fashion as previously reported.[30,31] In essence, cyanoxyl radicals were generated by an electron-transfer reaction between cyanate anions from a

sodium cyanate aqueous solution and aryl-diazonium salts, which were prepared in situ through a diazotization reaction of arylamine in water. Cyanoxyl persistent radicals and aryl-type active radicals were simultaneously produced, where only the latter species was capable of initiating chain growth, thus facilitating the copolymerization of *N*-acryloyl-glycosylamine glycomonomers (Glyco-AM) and free acrylamide (AM).[30,31] Particularly, glycocopolymers (i.e., AM/Glyco-AM) expressing different densities of carbohydrate ligands (i.e., *y/x*) were synthesized by varying the ratios between *N*-acryloyl-glycosylamine glycomonomers and free acrylamide. Lact-homopolymers of various chain lengths *n* was synthesized by varying the amount of *N*-lactosylacrylamide monomer without inclusion of free acrylamide. The oxidation of homopolymer Lact-AM 53 was performed by dissolving 10 mg of polymers in a total volume of 1 mL solution of 0.03 mol/L sodium periodate in DI nanopure water. The mixture was protected from light and stirred overnight at room temperature for reaction followed by 48 h of dialysis. The purified oxidized Lact-AM 53 (i.e., Lact-AM 53-Ox) homopolymer was freeze-dried for SWCNT dispersion.

Aqueous Dispersion and Characterization of Glycopolymer-SWCNT Complexes. Pristine CoMoCat SWCNT powder (SG65i grade, lot no. SG65i-L39), that is enriched in small diameter (6,5) chirality species, was purchased from CHASM Advanced Materials. SWCNT powder was dispersed in a total volume of 1 mL aqueous solutions of synthetic glycopolymers by tip sonication (model VCX 130, Sonics and Materials, Inc.) in an ice bath for 40 min at a power level of 8 W using a 2-mm diameter probe. The SWCNT:glycopolymer mass ratio was 1:4 for all dispersions, with the SWCNT concentration being either 0.1 or 0.25 mg/mL. Specifically, 0.25 mg/mL SWCNTs were dispersed in AM/Lact-AM copolymers that are denoted as 4:1, 17:1, 20:1, and 25:1 due to the availability of enough quantities of synthetic polymers. The rest of the

dispersions was prepared using 0.1 mg/mL SWCNTs. Supernatant dispersions were collected after 90 min centrifugation at 17,000 g and 19 ºC in 100 µL aliquots and used as stock samples. The differences in starting SWCNT quantities in four Lact-copolymers mentioned above were accounted for by dividing absorbance values across the entire spectral wavelengths by 2.5 when comparing the dispersion outcome of various Glyco-SWCNT complexes. The capability of each glycopolymer in dispersing SWCNTs was examined by producing three repeats of each sample. In addition, 0.36 mg/mL free sugar β-lactose, 0.04 mg/mL polyacrylamide (PAM) backbone (MW 44.7 kDa), and their mixtures of 0.36 mg/mL free sugar-0.04 mg/mL PAM were tested for stabilizing 0.1 mg/mL SWCNTs in water.

Optical spectroscopy characterization including vis-NIR absorbance and NIR fluorescence measurements were performed on a NS3 NanoSpectralyzer (Applied NanoFluorescence, LLC) using a 10 mm path length quartz cuvette. A fixed excitation wavelength of 532 nm laser was used for acquiring NIR fluorescence spectra. The concentration of SWCNTs in aqueous glycopolymer solutions was calculated using an extinction coefficient of 0.02554 L mg^{-1} cm^{-1} at 800 nm wavelength.[36] All samples were diluted by 10 times in DI water for spectroscopy measurements unless indicated otherwise.

Interactions of Glycopolymer Coatings with Surfactants and DNA. Sodium deoxycholate (SDC) (98%, BioXtra) and sodium dodecyl sulfate (SDS) used for glycopolymer/surfactant interactions were acquired from Sigma-Aldrich. Single-stranded DNA, $(GT)_{20}$ sequence, used for glycopolymer/DNA interactions was purchased from Integrated DNA Technologies. Stock solutions of 10 mass% SDS, SDC, and DNA, respectively, were prepared for glycopolymer coating modulation at room temperature. Initially, stock SWCNT samples prepared in glycopolymers (i.e., AM/Lact-AM 4:1 copolymer and Lact-AM 415 homopolymer)

were diluted with a factor of 10× in DI water. Then a small aliquot of 3 μL solutions of dispersing agents (i.e., SDS, SDC, and DNA) was added to 300 μL of diluted glyco-SWCNT samples, respectively, to obtain a final concentration of 0.1 mass% dispersing molecules. The mixtures were bath sonicated for 1 hour at room temperature for optical spectroscopy characterization. In addition, aqueous dispersions of 0.4 mg/mL $(GT)_{20}$ - 0.1 mg/mL SWCNTs were prepared by tip sonication in an ice bath for 40 min at a power level of 8 W and supernatant dispersions were collected after centrifugation at 17,000 g for 90 min. The stock supernatant samples of $(GT)_{20}$-SWCNTs were diluted with a factor of 10× in DI water. Then a small aliquot of 3 μL aqueous solutions of 10 mass% glycopolymers (i.e., AM/Lact-AM 4:1 copolymer and Lact-AM 415 homopolymer) were added to a 300 μL sample of diluted $(GT)_{20}$-SWCNTs, respectively, to obtain a final concentration of 0.1 mass% polymers. The mixture was bath sonicated for 1 hour at room temperature for DNA/glycopolymer coating interaction experiments.

RESULTS AND DISCUSSION

Early work on dispersions of carbohydrate-coated SWCNTs has demonstrated the wrapping of nanotubes by natural polysaccharides with glucose units, such as schizophyllan, curdlan, amylose, and starch.[15,29,37,38] Dispersions of SWCNTs by these polysaccharides often required the activation of helical structure formation by complexing with iodine or modulating the solvent property, such as adding dimethyl sulfoxide in water. These glucose-containing polysaccharides adsorbed on SWCNTs *via* van der Waals interactions and formed ordered, helical structures through interactions of the hydrophobic face of the pyranose rings (i.e., the 2-OH side of the glucose unit) and the hydrophobic surface of nanotube.[27,39] Furthermore, the helical conformation of

polysaccharides was potentially stabilized by hydrogen-bonds formed between adjacent residues.[27] Based on these previously known stabilization approaches of SWCNTs by polysaccharides, we examined the capability of synthetic glycopolymers with monosaccharide and disaccharide groups in dispersing nanotubes in water (Figure 1a). Two types of glycopolymers were investigated in this work: ten copolymers from acrylamide (AM) and glycosylacrylamide monomers (i.e., AM/Glyco-AM) and four homopolymers from lactosylacrylamide (i.e., Lact-AM) monomer only. Table 1 lists the glycopolymers used for producing aqueous dispersions of SWCNTs in this work. For copolymers, four of them are monosaccharide-containing polymers synthesized from D-galactose (Gal), D-glucose (Glc), *N*-acetyl-D-glucosamine (GlcNAc), and D-mannose (Man), respectively. Six disaccharide-containing copolymers were synthesized from β-lactose (Lact), which contains both Glc and Gal, to produce polymers with various sugar densities (i.e., *y/x* ratios of Lact-AM and AM units) and polymer chain lengths (i.e., repeating unit *n*). In addition, Lact-homopolymers with four different chain lengths were synthesized to elucidate the role of polymer length on stabilizing SWCNTs while maintaining a constant sugar density.

Table 1. List of glycopolymers used for producing aqueous dispersions of SWCNTs.

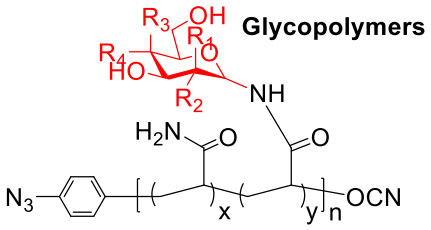

Glc, R_1 = H, R_2 = OH, R_3 = H, R_4 = OH
GlcNAc, R_1 = H, R_2 =NHAc, R_3 = H, R_4 = OH
Gal, R_1 = H, R_2 = OH, R_3 = OH, R_4 = H
Man, R_1 = OH, R_2 = H, R_3 = H, R_4 = OH
Lact, R_1 = H, R_2 = OH, R_3 = H, R_4 = *O*-Gal

Glycopolymers	**Abbreviations**	**Polymer Characterization**			
		Acrylamide *x*	Glycosylacrylamide *y*	Chain Length *n*	MW[*1] (Da)
Glc-copolymer	-	3	1	50	23.3k
Man-copolymer	-	4	1	87	44.2k
Gal-copolymer	-	4	1	50	26.8k
GlcNAc-copolymer	-	6	1	63	44.2k
Lact-copolymer (25:1)	AM/Lact-AM 25:1	25	1	53	112.6k
Lact-copolymer (20:1)	AM/Lact-AM 20:1	20	1	25	44.6k
Lact-copolymer (17:1)	AM/Lact-AM 17:1	17	1	29	45.7k
Lact-copolymer (7:1)	AM/Lact-AM 7:1	7	1	5	4.9k
Lact-copolymer (4:1)	AM/Lact-AM 4:1	4	1	2	1.5k
Lact-copolymer (1:2)	AM/Lact-AM 1:2	1	2	5	4.5k
Lact-homopolymer (0:9)	Lact-AM 9	0	1	9	3.7k
Lact-homopolymer (0:53)	Lact-AM 53	0	1	53	21.1k
Lact-homopolymer (0:85)	Lact-AM 85	0	1	85	33.7k
Lact-homopolymer (0:415)	Lact-AM 415	0	1	415	164.1k

[*1]. Average molecular weight determined by ^{1}H NMR spectrum of the glycopolymer

Glycopolymer-wrapped SWCNT complexes (Glyco-SWCNTs) were prepared by probe tip sonication of SWCNTs in aqueous solutions of glycopolymers above. Dispersions of each Glyco-SWCNT sample were performed in three repeats. For SWCNTs prepared in aqueous solutions of monosaccharides-containing copolymers, nanotubes formed pellets upon centrifugation resulting in clear supernatant solutions (Figure 1b). It is noteworthy to mention that Glc-copolymer produced a SWCNT dispersion of faint grayish color, however, the dispersion outcome was not significant. In addition, copolymers with other monosaccharides (Gal, GlcNAc, Man) did not

result in effective dispersions of SWCNTs in water. Interestingly, when a disaccharide Lact-copolymer (i.e., AM/Lact-AM 17:1) was utilized, we consistently obtained dark supernatant dispersions of SWCNTs in water (Figure 1b). We found that the identity of carbohydrate groups plays an important role in encapsulating SWCNTs because a glycopolymer with Lact residue composed of Glc and Gal stabilized nanotubes while those with monosaccharide Glc and Gal, respectively, did not produce stable dispersions of SWCNTs (Figure S1). We speculated that the disaccharide Lact potentially makes glycopolymers less flexible and imposes a special wrapping conformation on the nanotube surface while promoting multivalent interactions between hydrophobic faces of sugar rings and the hydrophobic surface of SWCNTs (Figure 1c).

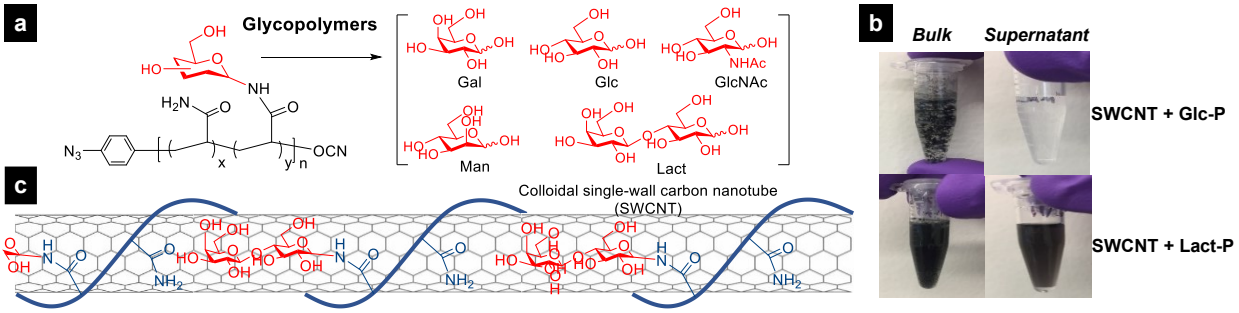

Figure 1. Glycopolymers and Glyco-SWCNT complexes. (**a**) Chemical structures of glycopolymers with monosaccharide and disaccharide. (**b**) Photographs of bulk dispersions without centrifugation and supernatants collected after centrifugation of SWCNT samples tip sonicated in Glc- and Lact-copolymers. (**c**) Helical wrapping of a SWCNT by Lact-copolymers.

The corresponding absorbance and fluorescence spectra of aqueous dispersions of SWCNTs in Lact-copolymer (i.e., AM/Lact-AM 17:1) showed characteristic optical transition peaks of nanotubes (Figure 2 and Figure S1). Particularly, E_{11} and E_{22} transition peak features of semiconducting tubes were clearly shown for Lact-SWCNT complexes in Figure 2a. These sharp,

discrete absorption peaks obtained for Lact-SWCNTs, compared with little to no absorption peaks obtained for nanotubes in monosaccharide-containing copolymers, are indicative of uniform dispersions of SWCNTs stabilized by Lact-copolymers. In addition, well-dispersed Lact-SWCNTs exhibited nanotube photoluminescence in the NIR region indicating individually dispersed nanotubes in water (Figure 2b). Although optical transition peaks with low absorbance values were observed for one Glc-SWCNT sample, other dispersion trials resulted in samples without clear peak features in both absorption and fluorescence spectra, similar to those obtained from SWCNTs prepared in other copolymers with monosaccharide (Figure 2). In addition, we examined capabilities of free sugar β-lactose, PAM backbone as well as a mixture of free β-lactose and PAM in dispersing SWCNTs, however, none of them resulted in aqueous dispersions of nanotubes (Figure S1). Consequently, we selected Lact-polymers to study the roles of carbohydrate identity and specific polymer characteristics in stabilizing SWCNTs in aqueous environments.

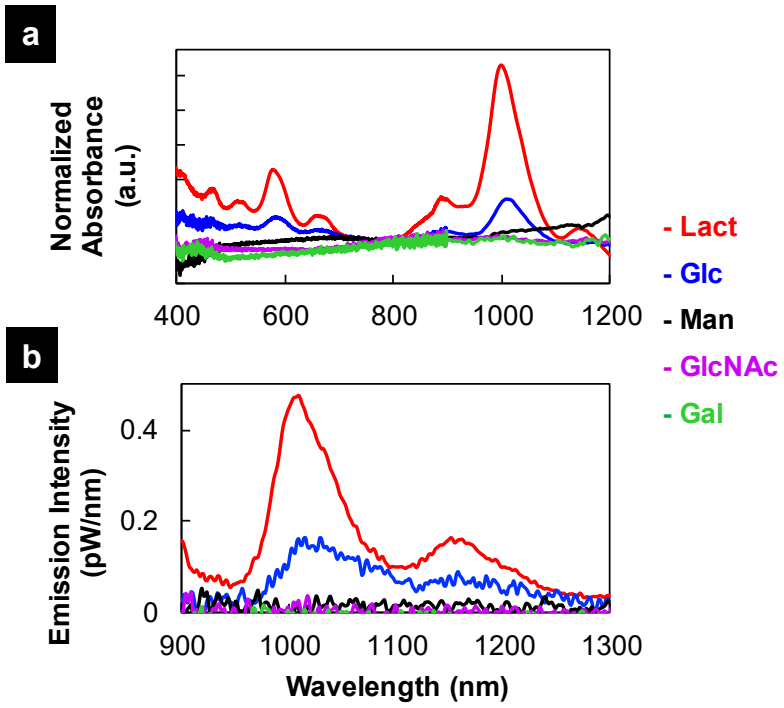

Figure 2. Optical characterization of Glyco-SWCNT samples. (**a**) Normalized absorbance spectra and (**b**) the corresponding fluorescence spectra of SWCNT samples prepared in aqueous solutions of copolymers with monosaccharide (Gal, Glc, GlcNAc, Man) and disaccharide (Lact). Before normalization, both absorbance and fluorescence values across the entire spectral wavelengths for Lact-SWCNTs were divided by 2.5 to account for the difference in nanotube concentration used in initial dispersions. Lact-copolymer used here is AM/Lact-AM 17:1.

Specifically, we created a library of lactose-containing polymers to further investigate the important roles of carbohydrate ligand density and polymer chain length in effectively stabilizing SWCNTs in water (Figure 3). The resulting Glyco-SWCNT complexes exhibited nanotube photoluminescence in the NIR. Absorbance and fluorescence spectra of various complexes are shown in Figure S2 and Figure S3. In general, we observed enhanced dispersion quality and yield of SWCNTs as a function of increasing sugar density when Lact-copolymers (AM/Lact-AM) with different sugar densities, *y/x*, were used to stabilize SWCNTs (Figure 3a). These are indicated by the narrowing of spectral line widths of absorption transition peaks and stronger intensities of Glyco-SWCNTs obtained in Lact-copolymers with higher sugar densities. Subsequently, we

plotted absorbance values of the maximum E_{11} peaks at wavelengths ranging from 998 to 1010 nm for various Glyco-SWCNT dispersions as a function of sugar density (Figure 3b and Figure S2). We observed a monotonic increase in absorbance values at the maximum E_{11} peak with increasing sugar density for SWCNT samples dispersed by Lact-copolymers, indicating an increase in the dispersion yield of nanotubes. Particularly, two Lact-copolymers, 25:1 and 20:1, with the lowest sugar density *y*/*x* values of 0.04 and 0.05, respectively, did not disperse SWCNTs despite their long polymer chain lengths of *n* being 53 and 25, respectively. On the other hand, the two highest dispersion yields of SWCNTs were obtained for Lact-copolymers, 7:1 and 1:2, regardless of their short polymer chain length (i.e., $n = 5$), due to their high sugar densities (i.e., $y/x = 0.14$ and 2, respectively). Specifically, AM/Lact-AM 1:2 polymer stabilized roughly 32.7 ± 14.0 mg/L SWCNTs in water, which corresponds to a dispersion yield of ≈ 33% of the starting SWCNT material. However, an exception from this general trend was observed for SWCNT samples using the AM/Lact-AM 4:1 polymer, the short chain length ($n = 2$) of which likely hindered the effective dispersion of nanotubes *via* the formation of helical wrapping despite its relatively high sugar density (i.e., $y/x = 0.25$). These findings suggest that a glycopolymer with a polymer chain length of as small as $n = 5$ can effectively stabilize SWCNTs *via* wrapping around a nanotube, given that the specific polymer contains a sufficient amount of sugar density. These results provide important insights into the synergistic effects of carbohydrate ligand identity (i.e., sugar unit and density) and polymer chain length of glycopolymers in creating stable Glyco-SWCNT complexes in aqueous environments.

Based on this observation, we next investigated the effect of homopolymer chain length on stabilizing SWCNTs in water using Lact-homopolymers while maintaining the sugar density (Figure 3c,d and Figure S3). As shown in Figure 3c, changes of normalized absorbance spectra

were observed for aqueous dispersions of SWCNTs by Lact-homopolymers with different chain lengths of *n* ranging from 9 to 415. Specifically, SWCNTs stabilized by homopolymers Lact-AM 85 and 415 (longer chain lengths n = 85 and 415) exhibited narrower spectral line widths and stronger peak intensities at the maximum E_{11} peak, indicating well-dispersed Glyco-SWCNT complexes. We further observed a sharp increase of absorbance values at the maximum E_{11} peaks for Glyco-SWCNTs as a function of increasing polymer chain length up to n = 85, followed by a minor increase in absorbance value with n = 415 (Figure 3d). This indicates that the formation of an ordered folding structure of Lact-homopolymer on the nanotube surface is enhanced with increasing polymer chain length up to roughly n = 85, after which the dispersion efficiency of SWCNTs remains relatively stable. The concentration of nanotubes in aqueous dispersions of SWCNTs stabilized by Lact-AM 415 was determined to be 37.6 ± 7.0 mg/L, corresponding to a nanotube dispersion yield of ≈ 38%. We also observed no obvious changes in absorption peak features of SWCNT samples over a period of five weeks, indicating the long-term stability of nanotubes stabilized by Lact-AM 415 in water (Figure S4).

It was reported that the hydrophobic interaction between the carbohydrate pyranose rings and the surface of nanotubes contributes in stabilizing SWCNTs by polysaccharides.[28] Therefore, a preliminary study to break the pyranose ring in Lact-AM 53 homopolymer by periodate was investigated. Briefly, carbohydrate residues in solutions of glycopolymers were chemically oxidized by sodium periodate (30 mM) in deionized (DI) H_2O at room temperature overnight. After reaction, excess periodate was removed by dialysis against DI H_2O and the reaction solution was lyophilized to obtain oxidized Lact-AM 53 (i.e., 53-Ox). Absorbance values at the maximum E_{11} peaks of SWCNTs dispersed by Lact-AM 53-Ox decreased slightly compared to those of nanotube samples in Lact-AM 53 (Figure 3d). This no significant change could be due to the

incomplete oxidation of sugar rings of Lact-AM 53-Ox that has relatively long polymer chain length (i.e., n = 53), resulting in the slightly lower level of stabilization of SWCNTs *via* the remaining portion of carbohydrate ring structures. However, this does indicate that the hydrophobic interaction between the carbohydrate rings and the surface of nanotubes is one of many interactions involved in stabilizing SWCNTs by glycopolymers. Future work on utilizing oxidized glycopolymers of short chain length with a controlled degree of oxidation should be conducted to provide further insights on the effect of hydrophobic interactions exerted by sugar rings on stabilizing SWCNTs in aqueous environments. Together, our findings demonstrated the roles of carbohydrate identity and polymer chain length of glycopolymers on stabilizing SWCNTs in water through facilitating the helical wrapping conformation of polymers.

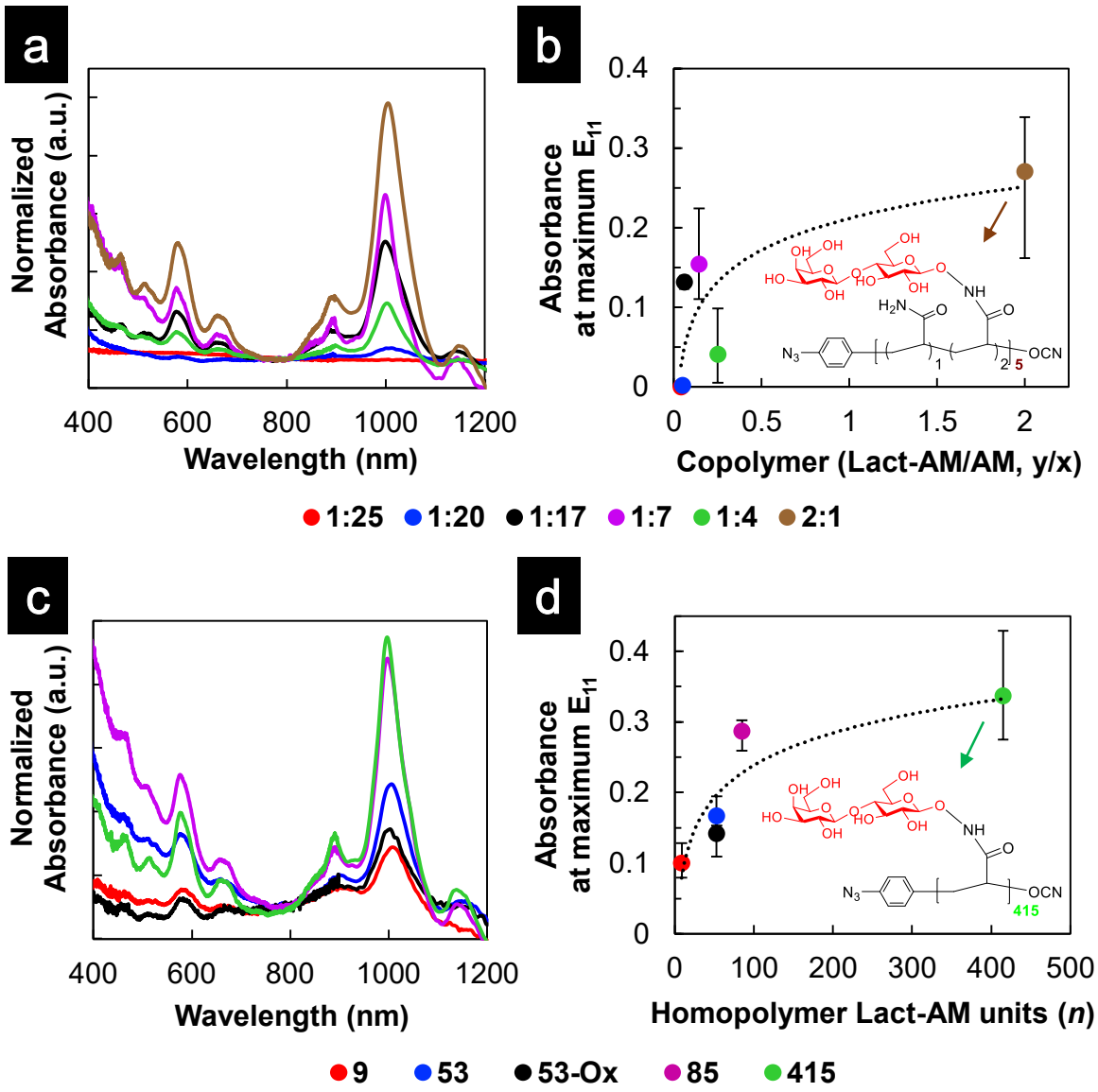

Figure 3. Optical characterization of aqueous dispersions of SWCNTs by Lact-glycopolymers with various Lact densities (i.e., *y*/*x*) and polymer chain lengths (i.e., *n*). (**a**) Normalized absorbance spectra and (**b**) absorbance values at the maximum E_{11} peak wavelength of SWCNT/Lact-copolymer samples as a function of Lact density in the copolymer. (**c**) Normalized absorbance spectra and (**d**) absorbance values at the maximum E_{11} peaks of SWCNT/Lact-homopolymer samples as a function of polymer chain length. Absorbance values in (**b**) and (**d**) were obtained from original spectra of stock samples that were diluted by a factor of 10× in DI water. As a guide for the eye, logarithmic fits were applied to the data. The error bars were obtained from minimum and maximum values of three repeats.

Furthermore, we investigated the strength of the interaction between SWCNTs and glycopolymers by measuring optical spectral changes of Glyco-SWCNTs upon addition of sodium deoxycholate (SDC), sodium dodecyl sulfate (SDS), and single-stranded DNA of $(GT)_{20}$, respectively (Figure 4). These molecules are often used to produce well-dispersed nanotubes in water through noncovalent complexation. Among these molecules, SDC is a surfactant known to bind strongly to the surface of SWCNTs and SDS is a weaker surfactant in coating nanotubes compared to SDC in an aqueous environment.[9,13] $(GT)_{20}$ DNA is a well-known recognition sequence that can effectively disperse and purify a specific SWCNT chirality species due to its ability to fold onto a nanotube to form a stable DNA-wrapped SWCNT hybrid.[21,22] Both SDC and SDS have been utilized previously to study the binding affinity of DNA sequences to SWCNTs through displacing DNA coatings by surfactants using absorption and fluorescence spectroscopy.[40–44] Particularly, measuring fluorescence spectral changes in the NIR has been proven to be an efficient way to probe the complexation affinity of a dispersing molecule and a nanotube. Various coating materials and solvents provide different local dielectric properties surrounding SWCNTs. The nanotube photoluminescence is highly sensitive in detecting small changes in the environmental dielectric constant in the form of spectral changes, such as solvatochromic shifts (i.e., spectral shift) and changes in spectral width and intensity.[45,46]

First, we investigated the surfactant effect with two Glyco-SWCNT complexes that were prepared from AM/Lact-AM 4:1 copolymer and Lact-AM 415 homopolymer, representing poorly and well-dispersed nanotubes, respectively. Particularly, SWCNTs dispersed in Lact-AM 415 homopolymer showed sharp absorption peaks indicating individually dispersed tubes. On the other hand, absorption peaks of SWCNT samples obtained in AM/Lact-AM 4:1 showed broader spectral line widths indicating small bundles and possible aggregations of nanotubes (Figure 4a

and 4b). Absorbance values at the maximum E_{11} peaks remained relatively stable when surfactants were added to Glyco-SWCNT samples. However, we found that SDC can effectively displace glycopolymer coatings from nanotubes in both Glyco-SWCNT complexes as indicated by the spectral blue shifts (i.e., decrease in wavelength) of the maximum E_{11} absorption peaks of nearly 8 and 15 nm, respectively for SWCNTs dispersed in Lact- copolymer and homopolymer (Figure 4c and 4d). Furthermore, the displacement of glycopolymer coatings from the surface of SWCNTs by SDC was clearly demonstrated by fluorescence spectroscopy which showed a spectral blue shift of nearly 21 nm and a 16.7-fold increase in emission intensity for SWCNTs dispersed in Lact- homopolymer as compared to a blue shift of roughly 13 nm and a 2.4-fold intensity increase for nanotube dispersions in Lact-copolymer (Figure 4e and 4f and Table S1). Particularly, the maximum E_{11} peak wavelength after displacing Lact-AM 415 coatings by SDC shifted to 985 nm corresponding to the E_{11} peak of SDC-coated (6,5) species, which is the most abundant nanotube species (i.e., ≈ 40 % of nanotube species) in the starting SWCNT material (Table S1).[21,44] The emission peaks obtained for SDC-coated SWCNTs after displacing Lact-AM 415 homopolymer are much sharper than those of nanotube samples obtained by replacing AM/Lact-AM 4:1 copolymer coatings. These observations suggest that starting from individually dispersed SWCNTs facilitates an efficient glycopolymer/surfactant exchange reaction and leads to an improved surface coverage of nanotubes by surfactant coatings. This is demonstrated by the significant increase in fluorescence intensity of SWCNTs after displacing Lact-AM 415 homopolymer, where nanotubes were protected from fluorescence quenching species in surrounding environments by SDC coatings. In comparison, no obvious changes were observed for absorption and fluorescence spectra of Glyco-SWCNT complexes after adding a weak

surfactant SDS, indicating that SDS was less likely to displace glycopolymer coatings on SWCNTs (Figure 4 and Table S1).

Then, we investigated with $(GT)_{20}$ DNA and observed a decrease of roughly 1.7-fold in fluorescence emission intensity at the maximum E_{11} peak for SWCNT samples prepared in AM/Lact-AM 4:1 copolymer when $(GT)_{20}$ DNA was added to Glyco-SWCNT complexes (Figure 4 and Table S1). The spectral changes in nanotube photoluminescence are caused by changes in dielectric environments of water surrounding nanotubes. The decrease in emission intensity is likely due to possible interactions between loosely bound AM/Lact-AM 4:1 copolymer coatings and DNA leading to the reduced surface coverage of SWCNTs and nanotube aggregations. However, we speculate that displacement of Lact-copolymer on the nanotube surface by DNA is not likely the case in this work. Oppositely, we prepared aqueous dispersions of $(GT)_{20}$-SWCNT hybrids and added AM/Lact-AM 4:1 copolymer and Lact-AM 415 homopolymer, respectively (Figure S5). As a result, no obvious changes were observed for absorbance spectra of $(GT)_{20}$-SWCNT samples upon adding glycopolymers. Surprisingly, SWCNT fluorescence measurements revealed a nearly 6.7-fold increase in emission intensity when Lact-AM 415 homopolymer was added to $(GT)_{20}$-SWCNTs, indicating that Lact-AM 415 binds to nanotube stronger than $(GT)_{20}$ DNA and further replace DNA coatings from the surface of SWCNTs (Figure S5d). This is also supported by the optical spectra of SWCNT samples obtained from direct dispersion in these two biopolymers. Specifically, nanotubes dispersed in Lact-AM 415 showed better dispersion quality exhibiting a sharper peak feature and higher emission intensity than that of $(GT)_{20}$-dispersed tubes (Figure S6).

Combined, our results suggest that the binding affinities of certain glycopolymers to SWCNTs could be similar to that of weak surfactant SDS as no obvious spectral changes were

observed after adding SDS in Glyco-SWCNT samples. Moreover, glycopolymers with proper structures could interact stronger with SWCNTs in water compared to well-known dispersants of nanotubes, including DNA. Our future work will focus on the rational design of glycopolymers with unique carbohydrate functionality and polymer structures, including the synthesis of glycopolymers with trisaccharide groups, for complexation with SWCNTs. The creation of stable, water-soluble Glyco-SWCNT complexes with distinct optical and carbohydrate functionalities will open many possibilities in biological and biomedical applications such as biochemical sensing and imaging advancement.

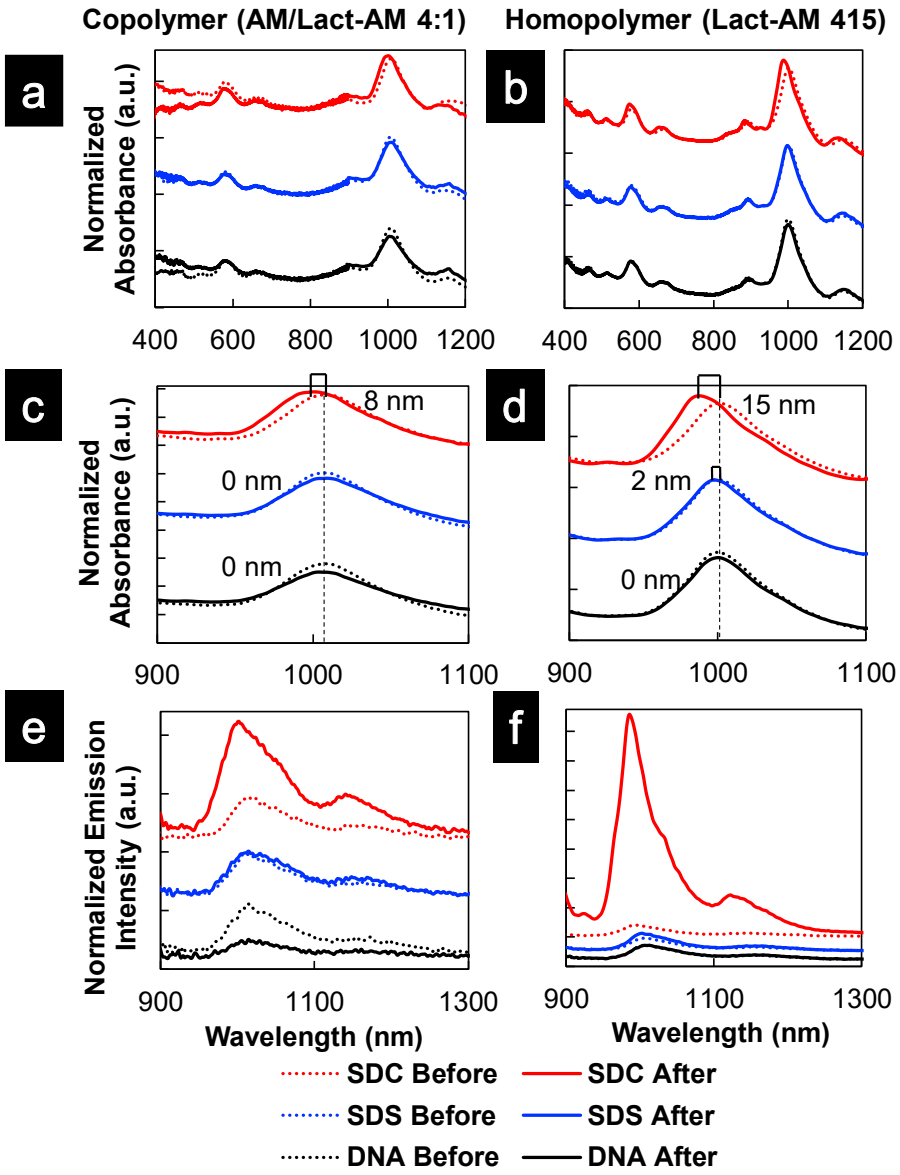

Figure 4. Optical characterization and different coating interactions of Glyco-SWCNT complexes prepared from copolymer (AM/Lact-AM 4:1) (**a**, **c**, **e**) and homopolymer (Lact-AM 415) (**b**, **d**, **f**)) with surfactants and DNA. Normalized absorbance spectra of SWCNTs complexed with (**a**) AM/Lact-AM 4:1 and (**b**) Lact-AM 415 before and after adding a final concentration of 0.1 mass % SDC, SDS, and $(GT)_{20}$ DNA, respectively, and (**c**,**d**) the corresponding spectra in the 900 to 1100 nm wavelength range. Normalized fluorescence spectra of SWCNTs complexed with (**e**) AM/Lact-AM 4:1 and (**f**) Lact-AM 415 before and after adding a final concentration of 0.1 mass % SDC, SDS, and $(GT)_{20}$ DNA, respectively.

CONCLUSIONS

In summary, we have demonstrated the complexation of glycopolymers and SWCNTs in water utilizing synthetic glycopolymers containing monosaccharide and disaccharide groups. Particularly, we investigated a range of monosaccharide- and disaccharide lactose-containing glycopolymers and revealed the synergistic effects of carbohydrate identity and polymer chain length on stabilizing SWCNTs in water. Glycopolymers with monosaccharide did not produce effective dispersions of SWCNTs. When disaccharide lactose was introduced, well-dispersed SWCNTs were obtained and the dispersion outcome was strongly dependent on both the sugar density and the polymer chain length. Moreover, Lact-copolymers with chain length as short as *n* being 5 enable the production of stable, water-solution Glyco-SWCNT complexes, given that the glycopolymer possess a sufficient amount of sugar density. The highest dispersion yield of SWCNTs was obtained in aqueous solutions of Lact-AM 415 homopolymer, which was found to be able to displace $(GT)_{20}$ DNA, a well-known dispersant of SWCNTs, from the surface of nanotubes. Taken together, this work demonstrated the important roles of both carbohydrate ligand identity and polymer chain lengths of glycopolymers in stabilizing SWCNTs through the formation of helical wrapping structures on the nanotube. The resulting stable, water-soluble Glyco-SWCNT complexes possess the intrinsic fluorescence properties of nanotubes. These findings offer important insights into designing biomimetic glycopolymers of specific structures and creating fluorescent, carbon-based nanocomplexes of distinct optical properties and carbohydrate functionalities for developing potential applications in biology.

ASSOCIATED CONTENT

Supporting Information.

The Supporting Information is available free of charge on the ACS Publications website.

Figures S1-S6, Table S1, and ^{1}H NMR spectra.

AUTHOR INFORMATION

Corresponding Author

*Emails: g.ao@csuohio.edu; x.sun55@csuohio.edu

ORCID

Geyou Ao: 0000-0002-9932-3971

Xue-Long Sun: 0000-0001-6483-1709

Author Contributions

The manuscript was written through contributions of all authors. All authors have given approval to the final version of the manuscript. †M.A.C. and K.K.C. contributed equally.

Notes

The authors declare no competing financial interest.

ACKNOWLEDGMENTS

We acknowledge support of Cleveland State University (CSU) for Faculty Start-Up Funds, Faculty Research Development Fund (FRD), Undergraduate Summer Research Award (USRA), and the grant from National Science Foundation (CBET-1917513).

REFERENCES

(1) Galassi, T. V.; Jena, P. V.; Shah, J.; Ao, G.; Molitor, E.; Bram, Y.; Frankel, A.; Park, J.; Jessurun, J.; Ory, D. S.; Haimovitz-Friedman, A.; Roxbury, D.; Mittal, J.; Zheng, M.; Schwartz, R. E.; Heller, D. A. An Optical Nanoreporter of Endolysosomal Lipid Accumulation Reveals Enduring Effects of Diet on Hepatic Macrophages in Vivo. *Sci. Transl. Med.* **2018**, *10*, eaar2680.

(2) Zhang, J.; Landry, M. P.; Barone, P. W.; Kim, J.-H.; Lin, S.; Ulissi, Z. W.; Lin, D.; Mu, B.; Boghossian, A. A.; Hilmer, A. J. Molecular Recognition Using Corona Phase Complexes Made of Synthetic Polymers Adsorbed on Carbon Nanotubes. *Nat. Nanotechnol.* **2013**, *8*, 959-968.

(3) Yi, H.; Ghosh, D.; Ham, M. H.; Qi, J.; Barone, P. W.; Strano, M. S.; Belcher, A. M. M13 Phage-Functionalized Single-Walled Carbon Nanotubes as Nanoprobes for Second near-Infrared Window Fluorescence Imaging of Targeted Tumors. *Nano Lett.* **2012**, *12*, 1176–1183.

(4) Chen, Y.; Star, A.; Vidal, S. Sweet Carbon Nanostructures: Carbohydrate Conjugates with Carbon Nanotubes and Graphene and Their Applications. *Chem. Soc. Rev.* **2013**, *42*, 4532–4542.

(5) Hasan, M. T.; Campbell, E.; Sizova, O.; Lyle, V.; Akkaraju, G.; Kirkpatrick, D. L.; Naumov, A. V. Multi-Drug/Gene NASH Therapy Delivery and Selective Hyperspectral NIR Imaging Using Chirality-Sorted Single-Walled Carbon Nanotubes. *Cancers (Basel).* **2019**, *11*, 1175.

(6) Nepal, D.; Balasubramanian, S.; Simonian, A. L.; Davis, V. A. Strong Antimicrobial Coatings: Single-Walled Carbon Nanotubes Armored with Biopolymers. *Nano Lett.* **2008**, *8*, 1896–1901.

(7) Hu, Y.; Liu, H.; Fang, C.; Li, C.; Xhyliu, F.; Dysert, H.; Bodo, J.; Habermehl, G.; Russell, B. E.; Li, W.; Chappell, M.; Jiang, X.; Ondrejka, S. L.; Hsi, E. D.; Maciejewski, J. P.; Yi, Q.; Anderson, K. C.; Munshi, N. C.; Ao, G.; Valent, J. N.; Lin, J.; Zhao, J. Targeting of CD38 by the Tumor Suppressor MiR-26a Serves as a Novel Potential Therapeutic Agent in Multiple Myeloma. *Cancer Res.* **2020**, 1077.

(8) Kwak, S. Y.; Lew, T. T. S.; Sweeney, C. J.; Koman, V. B.; Wong, M. H.; Bohmert-Tatarev, K.; Snell, K. D.; Seo, J. S.; Chua, N. H.; Strano, M. S. Chloroplast-Selective Gene Delivery and Expression in Planta Using Chitosan-Complexed Single-Walled Carbon Nanotube Carriers. *Nat. Nanotechnol.* **2019**, *14*, 447–455.

(9) Weisman, R. B.; Bachilo, S. M. Dependence of Optical Transition Energies on Structure for Single-Walled Carbon Nanotubes in Aqueous Suspension: An Empirical Kataura Plot. *Nano Lett.* **2003**, *3*, 1235–1238.

(10) Lin, C.-W.; Weisman, R. B. In Vivo Detection of Single-Walled Carbon Nanotubes: Progress and Challenges. *Future Medicine*, **2016**, *11*, 2885-2888.

(11) Strano, M. S.; Dyke, C. A.; Usrey, M. L.; Barone, P. W.; Allen, M. J.; Shan, H.; Kittrell, C.; Hauge, R. H.; Tour, J. M.; Smalley, R. E. Electronic Structure Control of Single-Walled Carbon Nanotube Functionalization. *Science.* **2003**, *301*, 1519–1522.

(12) Ju, S.-Y.; Kopcha, W. P.; Papadimitrakopoulos, F. Brightly Fluorescent Single-Walled Carbon Nanotubes via an Oxygen-Excluding Surfactant Organization. *Science.* **2009**, *323*, 1319–1323.

(13) Bachilo, S. M.; Strano, M. S.; Kittrell, C.; Hauge, R. H.; Smalley, R. E.; Weisman, R. B. Structure-Assigned Optical Spectra of Single-Walled Carbon Nanotubes. *Science.* **2002**,

298, 2361–2366.
(14) Chik, M. W.; Hussain, Z.; Zulkefeli, M.; Tripathy, M.; Kumar, S.; Majeed, A. B. A.; Byrappa, K. Polymer-Wrapped Single-Walled Carbon Nanotubes: A Transformation toward Better Applications in Healthcare. *Drug Deliv. Transl. Res*. **2019**, *9*, 578–594.
(15) Kim, O. K.; Je, J.; Baldwin, J. W.; Kooi, S.; Pehrsson, P. E.; Buckley, L. J. Solubilization of Single-Wall Carbon Nanotubes by Supramolecular Encapsulation of Helical Amylose. *J. Am. Chem. Soc.* **2003**, *125*, 4426–4427.
(16) Dohi, H.; Kikuchi, S.; Kuwahara, S.; Sugai, T.; Shinohara, H. Synthesis and Spectroscopic Characterization of Single-Wall Carbon Nanotubes Wrapped by Glycoconjugate Polymer with Bioactive Sugars. *Chem. Phys. Lett.* **2006**, *428*, 98–101.
(17) Budhathoki-Uprety, J.; Jena, P. V.; Roxbury, D.; Heller, D. A. Helical Polycarbodiimide Cloaking of Carbon Nanotubes Enables Inter-Nanotube Exciton Energy Transfer Modulation. *J. Am. Chem. Soc.* **2014**, *136*, 15545–15550.
(18) Roxbury, D.; Jagota, A.; Mittal, J. Sequence-Specific Self-Stitching Motif of Short Single-Stranded DNA on a Single-Walled Carbon Nanotube. *J. Am. Chem. Soc.* **2011**, *133*, 13545–13550.
(19) Roxbury, D.; Mittal, J.; Jagota, A. Molecular-Basis of Single-Walled Carbon Nanotube Recognition by Single-Stranded DNA. *Nano Lett.* **2012**, *12*, 1464–1469.
(20) Shankar, A.; Zheng, M.; Jagota, A. Energetic Basis of Single Wall Carbon Nanotube Enantiomer Recognition by Single Stranded DNA. *J. Phys. Chem. C* **2017**, *121*, 17497-17487.
(21) Ao, G.; Streit, J. K.; Fagan, J. A.; Zheng, M. Differentiating Left-and Right-Handed Carbon Nanotubes by DNA. *J. Am. Chem. Soc.* **2016**, *138*, 16677–16685.
(22) Ao, G.; Khripin, C. Y.; Zheng, M. DNA-Controlled Partition of Carbon Nanotubes in Polymer Aqueous Two-Phase Systems. *J. Am. Chem. Soc.* **2014**, *136*, 10383–10392.
(23) Tu, X.; Hight Walker, A. R.; Khripin, C. Y.; Zheng, M. Evolution of DNA Sequences toward Recognition of Metallic Armchair Carbon Nanotubes. *J. Am. Chem. Soc.* **2011**, *133*, 12998–13001.
(24) Roxbury, D.; Jena, P. V; Williams, R. M.; Enyedi, B.; Niethammer, P.; Marcet, S.; Verhaegen, M.; Blais-Ouellette, S.; Heller, D. A. Hyperspectral Microscopy of Near-Infrared Fluorescence Enables 17-Chirality Carbon Nanotube Imaging. *Sci. Rep.* **2015**, *5*.
(25) Prakrit Daniel E Roxbury, J. V. A Carbon Nanotube Optical Reporter Maps Endolysosomal Lipid Flux. *ACS Nano* **2017**, *11*, 10689–10703.
(26) Landry, M. P.; Ando, H.; Chen, A. Y.; Cao, J.; Kottadiel, V. I.; Chio, L.; Yang, D.; Dong, J.; Lu, T. K.; Strano, M. S. Single-Molecule Detection of Protein Efflux from Microorganisms Using Fluorescent Single-Walled Carbon Nanotube Sensor Arrays. *Nat. Nanotechnol.* **2017**, *12*, 368–377.
(27) Liu, Y.; Chipot, C.; Shao, X.; Cai, W. Edge Effects Control Helical Wrapping of Carbon Nanotubes by Polysaccharides. *Nanoscale* **2012**, *4*, 2584–2589.
(28) Liu, Y.; Chipot, C.; Shao, X.; Cai, W. Free-Energy Landscape of the Helical Wrapping of a Carbon Nanotube by a Polysaccharide. *J. Phys. Chem. C* **2011**, *115*, 1851–1856.
(29) Numata, M.; Asai, M.; Kaneko, K.; Bae, A. H.; Hasegawa, T.; Sakurai, K.; Shinkai, S. Inclusion of Cut and As-Grown Single-Walled Carbon Nanotubes in the Helical Superstructure of Schizophyllan and Curdlan (β-1,3-Glucans). *J. Am. Chem. Soc.* **2005**, *127*, 5875–5884.
(30) Tang, J.; Ozhegov, E.; Liu, Y.; Wang, D.; Yao, X.; Sun, X.-L. Straightforward Synthesis of

N-Glycan Polymers from Free Glycans via Cyanoxyl Free Radical-Mediated Polymerization. *ACS Macro Lett.* **2017**, *6*, 107–111.
(31) Chan, K. K.; Shi, Q.; Tang, J.; Sun, X.-L. Synthesis of Aryl Azide Chain-End Functionalized N-Linked Glycan Polymer and Its Photo-Labeling of Specific Proteins. *ACS Macro Lett.* **2020**, in revision (mz-2020-00210f)
(32) Sun, X.-L. Chemical Regulation of Glycosylation Processes. *Trends Glycosci. Glycotechnol.* **2018**, *30*, E179–E193.
(33) Zhang, H.; Ma, Y.; Sun, X. L. Recent Developments in Carbohydrate-Decorated Targeted Drug/Gene Delivery. *Med. Res. Rev*. **2010**, *30,* 270–289.
(34) Beck, A.; Wurch, T.; Bailly, C.; Corvaia, N. Strategies and Challenges for the next Generation of Therapeutic Antibodies. *Nat. Rev. Immunol.* **2010**, *10*, 345–352.
(35) El-Boubbou, K.; Huang, X. Glyco-Nanomaterials: Translating Insights from the "Sugar-Code" to Biomedical Applications. Curr. Med. Chem. **2011**, *18*, 2060-2078.
(36) Ivanova, M. V.; Lamprecht, C.; Jimena Loureiro, M.; Torin Huzil, J.; Foldvari, M. Pharmaceutical Characterization of Solid and Dispersed Carbon Nanotubes as Nanoexcipients. *Int. J. Nanomedicine* **2012**, *7*, 403–415.
(37) Alexander, S.; W., S. D.; R., H. J.; Fraser, S. J. Starched Carbon Nanotubes. *Angew. Chemie Int. Ed.* **2002**, *41*, 2508–2512.
(38) Numata, M.; Asai, M.; Kaneko, K.; Hasegawa, T.; Fujita, N.; Kitada, Y.; Sakurai, K.; Shinkai, S. Curdlan and Schizophyllan (β-1,3-Glucans) Can Entrap Single-Wall Carbon Nanotubes in Their Helical Superstructure. *Chem. Lett.* **2004**, *33*, 232–233.
(39) Miyoshi, K.; Uezu, K.; Sakurai, K.; Shinkai, S. Proposal of a New Hydrogen-Bonding Form to Maintain Curdlan Triple Helix. *Chem. Biodivers.* **2004**, *1*, 916–924.
(40) Zheng, Y.; Bachilo, S. M.; Weisman, R. B. Enantiomers of Single-Wall Carbon Nanotubes Show Distinct Coating Displacement Kinetics. *J. Phys. Chem. Lett.* **2018**, *9*, 3793–3797.
(41) Jena, P. V; Safaee, M. M.; Heller, D. A.; Roxbury, D. DNA-Carbon Nanotube Complexation Affinity and Photoluminescence Modulation Are Independent. *ACS Appl. Mater. Interfaces* **2017**, *9*, 21397-21405.
(42) Roxbury, D.; Tu, X.; Zheng, M.; Jagota, A. Recognition Ability of DNA for Carbon Nanotubes Correlates with Their Binding Affinity. *Langmuir* **2011**, *27*, 8282–8293.
(43) Kato, Y.; Inoue, A.; Niidome, Y.; Nakashima, N. Thermodynamics on Soluble Carbon Nanotubes: How Do DNA Molecules Replace Surfactants on Carbon Nanotubes? *Sci. Rep.* **2012**, *2*, 1–7.
(44) Xhyliu, F.; Ao, G. Chirality-Pure Carbon Nanotubes Show Distinct Complexation with Recognition DNA Sequences. *Carbon,* **2020**, *167*, 601-608.
(45) Nugraha, A. R. T.; Saito, R.; Sato, K.; Araujo, P. T.; Jorio, A.; Dresselhaus, M. S. Dielectric Constant Model for Environmental Effects on the Exciton Energies of Single Wall Carbon Nanotubes. *Appl. Phys. Lett.* **2010**, *97*, 091905.
(46) Choi, J. H.; Strano, M. S. Solvatochromism in Single-Walled Carbon Nanotubes. *Appl. Phys. Lett.* **2007**, *90*, 223114.

TOC